preprint SHEP-10-44
March 25, 2011

Muon Signals of Very Light CP-odd Higgs states of the NMSSM at the LHC

M. M. Almarashi and S. Moretti

School of Physics & Astronomy,
University of Southampton, Southampton, SO17 1BJ, UK

Abstract

We study here the $\mu^+\mu^-$ decay mode of a very light CP-odd Higgs boson of the NMSSM, a_1, produced in association with a bottom-antibottom pair and find that, despite small event rates, a significant signal should be extractable from the SM background at the LHC with high luminosity.

1 Introduction

In the Next-to-Minimal Supersymmetric Standard Model (NMSSM) [1], as a result of the introduction of an extra complex singlet scalar field, which only couples to the two MSSM-type Higgs doublets, the ensuing Higgs sector comprises a total of seven mass eigenstates: a charged pair $h^\pm$, three CP-even Higgses $h_{1,2,3}$ ($m_{h_1} < m_{h_2} < m_{h_3}$) and two CP-odd Higgses $a_{1,2}$ ($m_{a_1} < m_{a_2}$). Consequently, Higgs phenomenology in the NMSSM is plausibly different from that of the MSSM, i.e, the minimal realisation of Supersymmetry (SUSY).

In particular, over the past few years, there have been attempts to extend the so-called 'No-lose theorem' of the MSSM – stating that at least one MSSM Higgs boson should be observed via the usual SM-like production and decay channels at the Large Hadron Collider (LHC) throughout the entire MSSM parameter space [2] – to the case of the NMSSM [3, 4, 5]. From this perspective, it was realised that at least one NMSSM Higgs boson should remain observable at the LHC over the NMSSM parameter space that does not allow any Higgs-to-Higgs decay. However, when the only light non-singlet (and, therefore, potentially visible) CP-even Higgs boson, h_1 or h_2, decays mainly to two very light CP-odd Higgs bosons, $h_{1,2} \to a_1 a_1$, one may not have a Higgs signal of statistical significance at the LHC [6]. In

fact, further violations to the theorem may well occur if one enables Higgs-to-SUSY particle decays (e.g., into neutralino pairs, yielding invisible Higgs signals) [7, 8].

While there is no conclusive evidence on whether a 'No-lose theorem' can be proved for the NMSSM at the LHC, there has also been put forward an orthogonal approach: to see when a, so to say, 'More-to-gain theorem' for the LHC [9, 10, 11, 12] can be formulated within the NMSSM. That is, whether there exist regions of the NMSSM parameter space where more and/or different Higgs states of the NMSSM are visible at the LHC than those available within the MSSM.

In our attempt to overview both such possibilities, we consider here the case of the $\mu^+\mu^-$ decay channel of a light neutral CP-odd Higgs boson produced in association with b-quark pairs at the LHC. This work complements the one carried out in [12], which concentrated on $a_1 \to \tau^+\tau^-$ and $\gamma\gamma$ decays.

The plan of this paper is as follows. In Sect. 2 we describe the parameter space scans performed. In Sect. 3 we discuss inclusive event rates. In Sect. 4 we describe the signal-to-background analysis performed and introduce some benchmark points where an a_1 signal can be extracted via the $\mu^+\mu^-$ decay mode. Finally, in Sect. 5, we summarise and conclude.

2 Parameter Space Scan

For our study of the NMSSM Higgs sector we have used NMSSMTools [13, 14]. This package computes the masses, couplings and decay widths into two particle final states of all the Higgs bosons of the NMSSM in terms of its input parameters, which can be taken at either the Electro-Weak (EW) or grand unification scale. NMSSMTools also takes into account theoretical consistency as well as experimental limits from negative Higgs searches at LEP [15] and Tevatron[1], including the unconventional channels relevant for the NMSSM only.

Here, instead of postulating unification or taking into account the SUSY breaking mechanism, we fixed the soft SUSY breaking terms to a very high value, so that they give a small or no contribution at all to the outputs of the parameter scans. Consequently, we are left with six free parameters at the EW scale, uniquely defining the NMSSM Higgs sector at tree-level. Our parameter space is in particular defined through the Yukawa couplings λ and κ, the soft trilinear terms A_λ and A_κ, plus $\tan\beta$ (the ratio of the Vacuum Expectation Values (VEVs) of the two Higgs doublets) and $\mu_{\rm eff} = \lambda\langle S\rangle$ (where $\langle S\rangle$ is the VEV of the Higgs singlet).

In order to make a comprehensive study of the NMSSM parameter space, we have used the NMHDECAY code to scan over the aforementioned six parameters taken in the following intervals:

$$\lambda : 0.0001 - 0.7, \quad \kappa : 0 - 0.65, \quad \tan\beta : 1.6 - 54,$$
$$\mu : 100 - 1000 \text{ GeV}, \quad A_\lambda : -1000 - +1000 \text{ GeV}, \quad A_\kappa : -10 - 0.$$

Soft terms which are fixed in the scan include:

- $m_{Q_3} = m_{U_3} = m_{D_3} = m_{L_3} = m_{E_3} = 1$ TeV,

[1] Speculations of an excess at LEP which could be attributed to NMSSM Higgs bosons are found in [16]. Very light CP-odd Higgs bosons of the NMSSM could also be produced in some rare hadron decays [17]

- $A_{U_3} = A_{D_3} = A_{E_3} = 1.2$ TeV,
- $m_Q = m_U = m_D = m_L = m_E = 1$ TeV,
- $M_1 = M_2 = M_3 = 1.5$ TeV.

In line with the assumptions made in [3, 4], the allowed decay modes for the CP-odd neutral NMSSM Higgs boson a_1 are:

$$a_1 \to \mu^+\mu^-, \tau^+\tau^-, gg, s\bar{s}, c\bar{c}, b\bar{b}, t\bar{t}, \gamma\gamma, Z\gamma, \text{ sparticles}. \tag{1}$$

We have performed our scan over 10 millions of randomly selected points in the specified parameter space. The output, as stated earlier, contains masses, Branching Ratios (BRs) and couplings of the NMSSM Higgses, for all the points which have passed the various experimental and theoretical constraints. The points which violate the latter are automatically eliminated by NMSSMTools.

3 Inclusive Event Rates

The surviving data points are then used to determine the cross-sections for NMSSM Higgs hadro-production by using CalcHEP [18] and MadGraph [19][2], wherein some new modules have been implemented for this purpose [21]. As the SUSY mass scales have been arbitrarily set well above the EW one (see above), the NMSSM Higgs production modes exploitable in simulations at the LHC are those involving couplings to heavy ordinary matter only. Amongst the production channels onset by the latter, we focus here on

$$q\bar{q}, gg \to b\bar{b}\ a_1, \tag{2}$$

i.e., Higgs production in association with a b-quark pair.

As an initial step towards the analysis of the data, we have computed the production cross-section times the decay BR against each of the six parameters of the NMSSM, as intimated. We started by computing total (i.e., fully inclusive) rates. Figs. 1 and 2 present the results of our scan, the first series of plots illustrating the distribution of event rates over the six independent NMSSM parameters, m_{a_1} and as a function of the BR of the corresponding channel with the second plot displaying the correlations between the a_1 mass and the di-muon decay rate. It is clear that the large $\tan\beta$ and small $\mu_{\rm eff}$ (and, to some extent, also small λ) region is the one most compatible with current theoretical and experimental constraints, while the distributions in κ, A_λ and A_κ are rather uniform (top six panes in Fig. 1). From a close look at Fig. 2 it is further clear that the BR($a_1 \to \mu^+\mu^-$) can be of $\mathcal{O}(10\%)(\mathcal{O}(1\%))[\mathcal{O}(0.1\%)$ or less] when $2m_\mu < m_{a_1} < 2m_\tau (2m_\tau < m_{a_1} < 2m_b)[2m_b < m_{a_1}]$, respectively. The first region of parameter space ($m_{a_1} < 2m_\tau$) is rather small, the second one ($2m_\tau < m_{a_1} < 2m_b$) more significant, yet the widest one is the third one ($2m_b < m_{a_1}$). However, by looking at the two bottom panes of Fig. 1, it is remarkable to notice that the event rates are sizable in all such mass regions, topping the 10^4 fb level in the two lower

[2]We adopt herein CTEQ6L [20] as parton distribution functions, with scale $Q = \sqrt{\hat{s}}$, the centre-of-mass energy at parton level, for all processes computed.

mass intervals and the 10^3 fb level in the higher mass range. Finally, notice that the mass region below the $\mu^+\mu^-$ threshold is severly constrained [22].

4 Signal-to-Background Analysis

We perform here a partonic signal-to-background (S/B) analysis. We assume $\sqrt{s} = 14$ TeV throughout for the LHC energy. Also, in our numerical analyses, we have taken $m_b(m_b) = 4.214$ GeV and $m_t^{\rm pole} = 171.4$ GeV for the (running) bottom- and (pole) top-quark mass, respectively, while we have input $m_\tau^{\rm pole} = 1.777$ GeV and $m_\mu^{\rm pole} = 0.1057$ GeV for the (pole) tau- and (pole) muon-lepton mass, respectively. After implementing the following standard cuts

$$\Delta R(b,\bar{b}), \Delta R(b,\mu^+), \Delta R(\bar{b},\mu^+), \Delta R(b,\mu^-), \Delta R(\bar{b},\mu^-), \Delta R(\mu^+,\mu^-) > 0.4$$
$$|\eta(b)|, |\eta(\bar{b})|, |\eta(\mu^+)|, |\eta(\mu^-)| < 2.5$$
$$P_T(b), P_T(\bar{b}) > 20 \text{ GeV}, P_T(\mu^+), P_T(\mu^-) > 5 \text{ GeV}, \quad (3)$$

we obtain the invariant masses of the $\mu^+\mu^-$ system depicted in Figs. 3–7, where we show the combined yield of the signal induced by $q\bar{q}, gg \to b\bar{b}\mu^+\mu^-$ (via g and a_1 exchange) and of the irreducible background due to $q\bar{q}, gg \to b\bar{b}\mu^+\mu^-$ (via g, γ and Z exchange), including their interference. We also show in Figs. 3–7 the top-antitop reducible background, i.e., $q\bar{q}, gg \to t\bar{t} \to b\bar{b}W^+W^- \to b\bar{b}\mu^+\mu^- P_T^{\rm miss}$.

We notice the dominance of the $\gamma \to \mu^+\mu^-$ tail of the irreducible background at very small di-muon invariant masses. Furthermore, the reducible background starts reaching its maximum at around $M_W/2$. Finally, the $Z \to \mu^+\mu^-$ peak of the irreducible background becomes overwhelming already at 60 GeV or so. Overall, the $\mu^+\mu^-$ signal yield in such a mass region is of order 75 (for m_{a_1} reaching 60 GeV or so) to 1440 (for m_{a_1} starting at 10 GeV or so) signal events over a sizably smaller background (notice the logarithmic scale of the plots and notice that we are assuming, e.g., 300 fb^{-1} of accumulated luminosity).

While the number of events is not very large, there is potential scope to extract a significant signal over the above interval thanks to the high mass resolution that can be achieved using muon pairs. Assuming $\mu^+\mu^-$ resolutions of 1 GeV [23], we obtain as signal significances $S/\sqrt{B}$ (where S and B are the signal and background rates, respectively, after a given luminosity), as a function of such a luminosity, those depicted in Fig. 8 (left hand side). The corresponding signal event rates are found instead in the right hand side of the same figure. From these last results, it is clear that detection at the LHC could occur for a_1 masses between ≈ 10 and ≈ 40 GeV with rather modest luminosity, 30 fb^{-1} or so, while $\approx 50 (\approx 60)$ GeV masses require some 200(300) fb^{-1} while heavier states will not be resolvable even at the end of the LHC era.

5 Conclusions

Due to introducing a complex singlet superfield, the NMSSM can have a CP-odd Higgs boson with very low mass, a_1. We have proven that there exist sizable regions of the NMSSM parameter space where this kind of Higgs state, with a mixed singlet and doublet nature, could

potentially be detected at the LHC if 10 GeV $< m_{a_1} \leq 60$ GeV in the $a_1 \to \mu^+\mu^-$ mode if the CP-odd Higgs state is produced in association with a $b\bar{b}$ pair for large tanβ plus small $\mu_{\rm eff}$ and λ. After a realistic S/B analysis at parton level, we have in fact produced results showing that the extraction of light mass $a_1 \to \mu^+\mu$ resonances above both the irreducible and (dominant) reducible background should be feasible using standard reconstruction techniques [24, 25]. While more refined analyses, incorporating parton shower, hadronisation and detector effects, are needed in order to delineate the true discovery potential of the LHC over the actual NMSSM parameter space, we are confident that our results are a step in the right direction to both: (i) prove the existence of a 'More-to-gain theorem' at the CERN collider for the NMSSM with respect to the MSSM (as $\mu^+\mu^-$ signals from such light Higgs bosons are not at all possible in the latter scenario) and (ii) to establish a 'No-lose theorem' for the NMSSM at the LHC (as some of the parameter regions where the aforementioned signal can be detected overlap with those where $h_{1,2} \to a_1 a_1$ decays might be ineffective in extracting an h_1 signal).

Notice that we have explored here the three mass regimes $2m_\mu < m_{a_1} < 2m_\tau$, $2m_\tau < m_{a_1} < 2m_b$ and $2m_b < m_{a_1}$. The first interval in unresolvable because of a large irreducible background due to soft photons splitting into $\mu^+\mu^-$ pairs. The second one can actually be resolved only just below its upper end, i.e., close to the $2m_b$ threshold, above which a_1 state remains detectable for several tens of GeV. However, when $m_{a_1} > 60$ GeV, it is the combination of both the irreducible and reducible background induced by on-shell Z bosons that prevents detection.

Acknowledgments

This work is supported in part by the NExT Institute. M. M. A. acknowledges a scholarship granted to him by Taibah University (Saudi Arabia).

References

[1] For reviews, see: e.g., U. Ellwanger, C. Hugonie and A. M. Teixeira, Phys. Rept. **496** (2010) 1 (and references therein); M. Maniatis, Int. J. Mod. Phys. A **25** (2010) 3505 (and references therein).

[2] J. Dai, J.F. Gunion, R. Vega, Phys. Lett. B **315** (1993) 355 and Phys. Lett. B **345** (1995) 29; J.R. Espinosa, J.F. Gunion, Phys. Rev. Lett. **82** (1999) 1084.

[3] U. Ellwanger, J. F. Gunion and C. Hugonie, JHEP **0507** (2005) 041; U. Ellwanger, J.F. Gunion, C. Hugonie and S. Moretti, hep-ph/0305109 and hep-ph/0401228.

[4] U. Ellwanger, J.F. Gunion and C. Hugonie, hep-ph/0111179; D.J. Miller and S. Moretti, hep-ph/0403137; C. Hugonie and S. Moretti, hep-ph/0110241; A. Belyaev, S. Hesselbach, S. Lehti, S. Moretti, A. Nikitenko and C. H. Shepherd-Themistocleous,

arXiv:0805.3505 [hep-ph]; J. R. Forshaw, J. F. Gunion, L. Hodgkinson, A. Papaefstathiou and A. D. Pilkington, JHEP **0804** (2008) 090; A. Belyaev, J. Pivarski, A. Safonov, S. Senkin and A. Tatarinov, Phys. Rev. D **81** (2010) 075021.

[5] S. Moretti, S. Munir and P. Poulose, Phys. Lett. B **644** (2007) 241.

[6] D. Zerwas and S. Baffioni, private communication; S. Baffioni, talk presented at "GdR Supersymétrie 2004, 5-7 July 2004, Clermont-Ferrand, France.

[7] U. Ellwanger and C. Hugonie, Eur. Phys. J. C **25** (2002) 297.

[8] A. Djouadi *et al.*, JHEP **0807** (2008) 002.

[9] S. Moretti and S. Munir, Eur. Phys. J. C **47** (2006) 791.

[10] S. Munir, talk given at the 'International School of Subnuclear Physics, 43rd Course', Erice, Italy, August 29 – Sept. 7, 2005, to be published in the proceedings, preprint SHEP-05-37, October 2005.

[11] E. Accomando *et al.*, arXiv:hep-ph/0608079.

[12] M. M. Almarashi and S. Moretti, arXiv:1011.6547 [hep-ph].

[13] U. Ellwanger, J.F. Gunion and C. Hugonie, JHEP **0502** (2005) 066; U. Ellwanger and C. Hugonie, Comput. Phys. Commun. **175** (2006) 290.

[14] See http://www.th.u-psud.fr/NMHDECAY/nmssmtools.html.

[15] S. Schael *et al.*, Eur. Phys. J. C **47** (2006) 547.

[16] R. Dermisek and J. F. Gunion, Phys. Rev. D **76** (2007) 095006.

[17] X.G. He, J. Tandean and G. Valencia, JHEP **0806** (2008) 002; Phys. Rev. Lett. **98** (2007) 081802; Phys. Rev. D **74** (2006) 115015; Phys. Lett. B **631** (2005) 100.

[18] A. Pukhov, arXiv:hep-ph/0412191.

[19] T. Stelzer and W. F. Long, Comput. Phys. Commun. **81** (1994) 357.

[20] See http://hep.pa.msu.edu/cteq/public/cteq6.html.

[21] M. M. Almarashi and S. Moretti, private programs.

[22] S. Andreas, O. Lebedev, S. R. Sanchez and A. Ringwald, JHEP **1008** (2010) 003.

[23] See Sect. 11.2.2 of [25].

[24] ATLAS Collaboration, arXiv:0901.0512 [hep-ex].

[25] CMS Collaboration, J. Phys. G **34** (2007) 995.

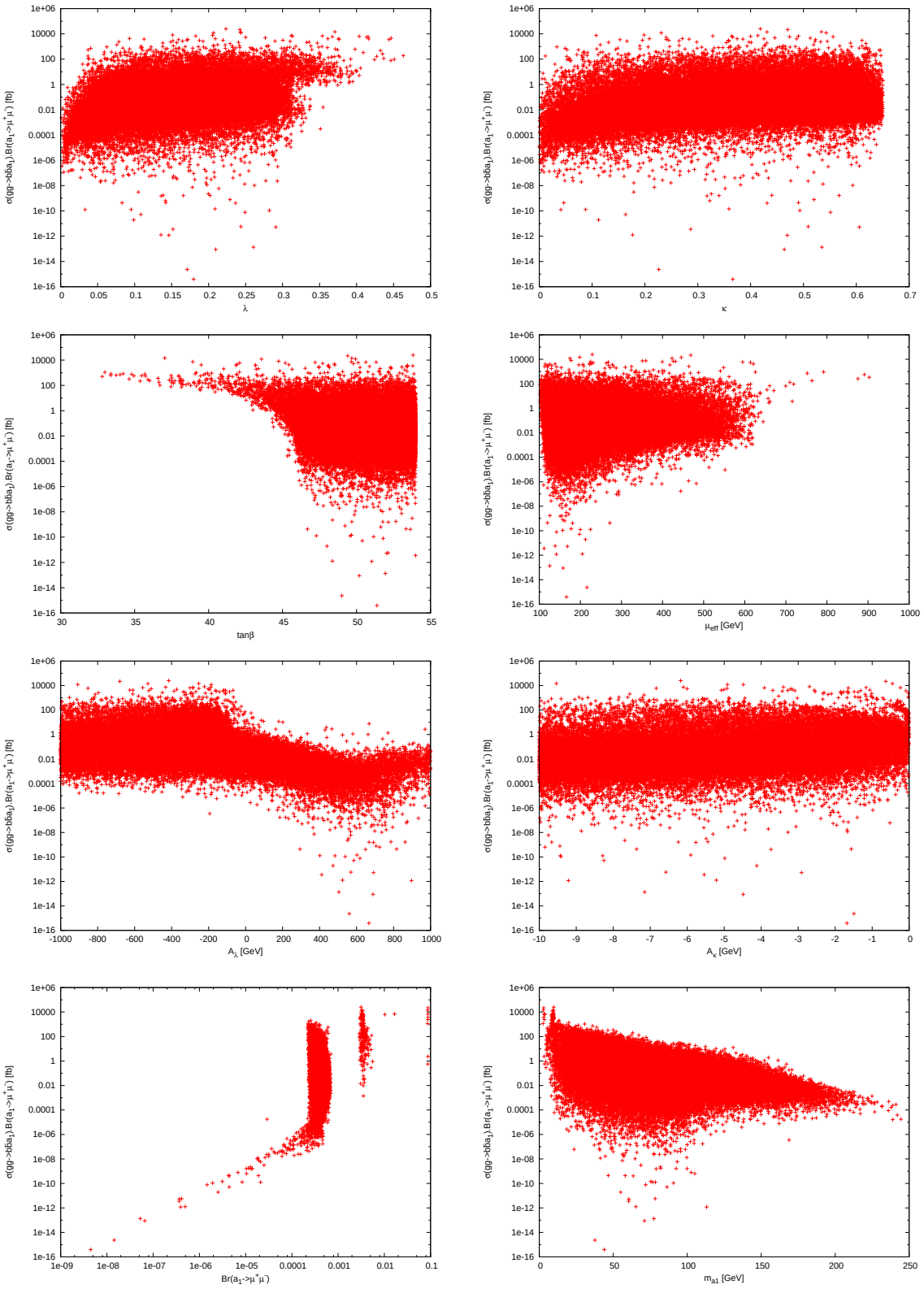

Figure 1: The rates for $\sigma(q\bar{q}, gg \to b\bar{b}a_1)$ BR$(a_1 \to \mu^+\mu^-)$ as a function of λ, κ, $\tan\beta$, $\mu_{\rm eff}$, A_λ, A_κ, BR$(a_1 \to \mu^+\mu^-)$ and m_{a_1}.

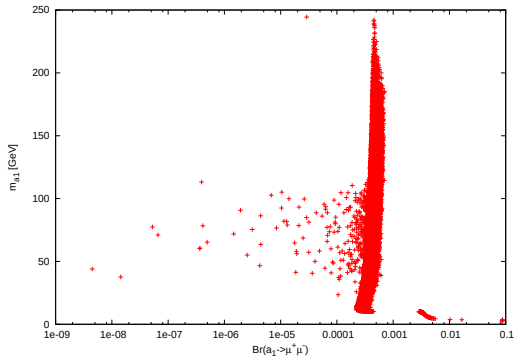

Figure 2: The CP-odd Higgs mass m_{a_1} as a function of BR($a_1 \to \mu^+\mu^-$).

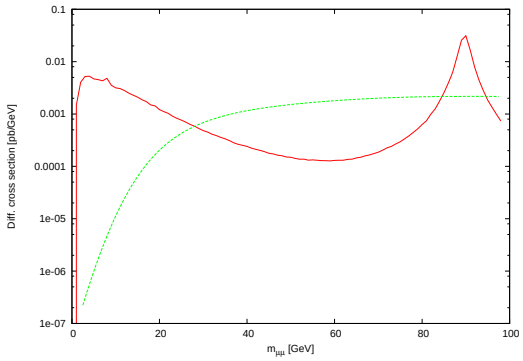

Figure 3: The differential cross section in the $\mu^+\mu^-$ channel for m_{a_1}=9.76 GeV as a function of $m_{\mu\mu}$, after the cuts in (3) with λ = 0.22341068, κ = 0.4184933, tanβ = 53.819484, μ = 228.94259, A_λ = -415.57365 and A_κ = -6.1773643. The solid line represents the signal and irreducible background together whereas the dashed line is the $t\bar{t}$ background. (Notice that here $2m_b^{\rm pole} > m_{a_1}$.)

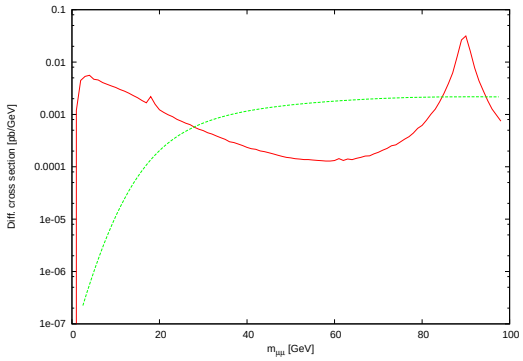

Figure 4: The differential cross section in the $\mu^+\mu^-$ channel for m_{a_1}=19.98 GeV as a function of $m_{\mu\mu}$, after the cuts in (3) with λ = 0.075946278, κ = 0.11543578, tanβ = 51.507125, μ = 377.4387, A_λ = -579.63592 and A_κ = -3.5282881. The solid line represents the signal and irreducible background together whereas the dashed line is the $t\bar{t}$ background.

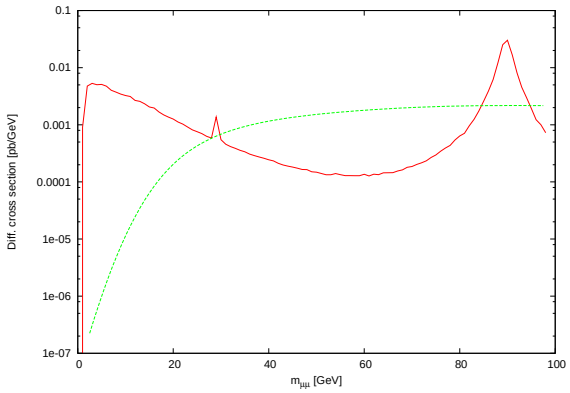

Figure 5: The differential cross section in the $\mu^+\mu^-$ channel for m_{a_1}=30.67 GeV as a function of $m_{\mu\mu}$, after the cuts in (3) with λ = 0.10861169, κ = 0.4654168, tanβ = 48.063727, μ = 222.99377, A_λ = -952.59787 and A_κ = -7.2147327. The solid line represents the signal and irreducible background together whereas the dashed line is $t\bar{t}$ background.

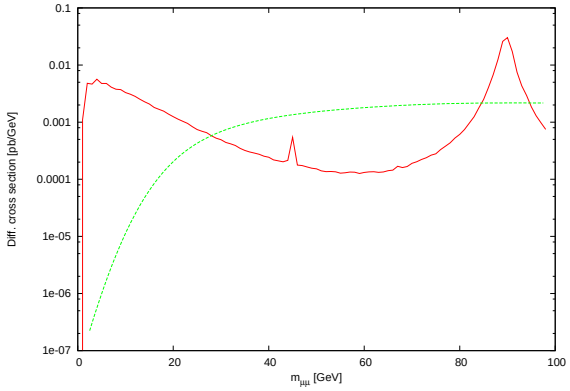

Figure 6: The differential cross section in the $\mu^+\mu^-$ channel for m_{a_1}=46.35 GeV as a function of $m_{\mu\mu}$, after the cuts in (3) with λ = 0.14088263, κ = 0.25219468, tanβ = 50.558484, μ = 317.07532, A_λ = -569.60665 and A_κ = -8.6099538. The solid line represents the signal and irreducible background together whereas the dashed line is the $t\bar{t}$ background.

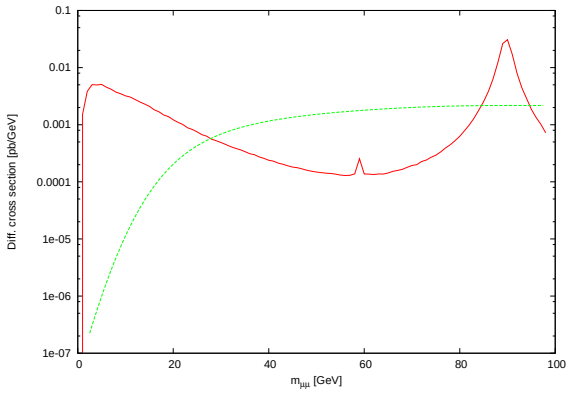

Figure 7: The differential cross section in the $\mu^+\mu^-$ channel for m_{a_1}=60.51 GeV as a function of $m_{\mu\mu}$, after the cuts in (3) with λ = 0.17410656, κ = 0.47848034, tanβ = 52.385408, μ = 169.83139, A_λ = -455.85097 and A_κ = -9.0278415. The solid line represents the signal and irreducible background together whereas the dashed line is the $t\bar{t}$ background.

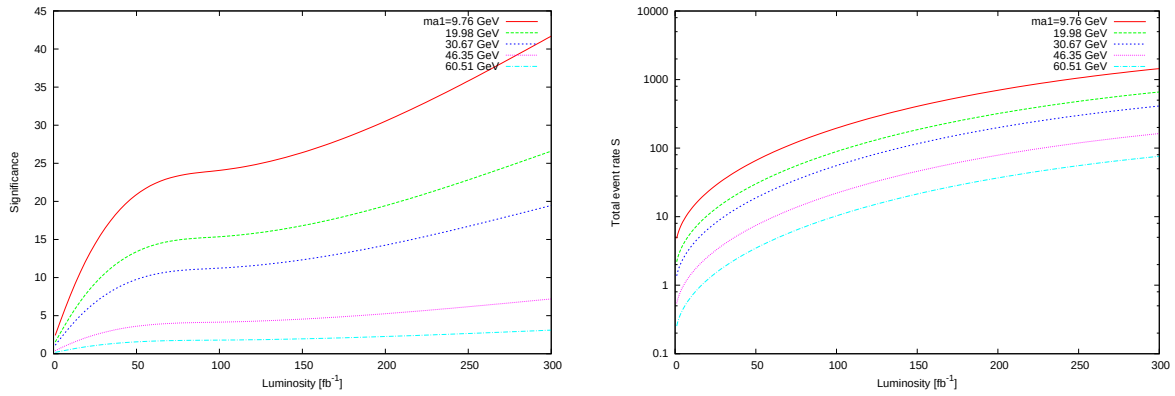

Figure 8: The significance $S/\sqrt{B}$ (left) and total event rate S (right) of the $q\bar{q}, gg \to b\bar{b}a_1 \to b\bar{b}\mu^+\mu^-$ signal as a function of the integrated luminosity.